

Surface functionalisation of porous silicon using 3-Aminopropyl triethoxy silane (APTS)

Dr Shalini Singh¹

¹Department of Zoology, GDC, Kuchlai, Sitapur, Uttar Pradesh

Received: 21 July 2023 Accepted & Reviewed: 25 July 2023, Published: 31 July 2023

Abstract

Porous silicon (p-Si) has emerged as a versatile material with immense potential in biomedical, optical, and sensor applications due to its high surface area and tunable surface chemistry. However, to fully exploit its capabilities, surface modification is essential to enhance its chemical stability and functional performance. This study focuses on the surface functionalisation of p-Si using 3-Aminopropyltriethoxysilane (APTS), a silane coupling agent known for introducing amine functionalities onto silicon-based surfaces. The process involves the hydrolysis and condensation of APTS molecules, forming covalent Si–O–Si bonds with the p-Si surface, resulting in a stable organosilane layer. The presence of terminal amine groups facilitates further conjugation with biomolecules or nanostructures, broadening the applicability of p-Si in areas such as biosensing, drug delivery, and nanoelectronics. The study also explores the characterization techniques employed—such as FTIR, contact angle measurements, and SEM/AFM imaging—to confirm successful functionalisation and understand the morphology and surface chemistry alterations. The findings demonstrate that APTS treatment is an effective strategy for enhancing the functional versatility of porous silicon surfaces.

Keywords:- Porous Silicon (p-Si), Surface Functionalisation, Aminopropyltriethoxysilane (APTS), Silanization, Amine Functional Groups, Covalent Bonding, Biosensors, Surface Characterization, Nanotechnology, Biomedical Applications

Introduction

The present study explain a simple silanization reaction to modify/functionalise nanostructured porous silicon surface preapred at different current densities to obtain different pore sizes. This functionalized surface can be exploit for further use in biosensors, target drug delivery and nanomedicine.

The desirability of constructing silicon-based optoelectronic devices and chemical and biological sensors has prompted considerable developments in the surface chemistry of luminescent porous silicon (PS) [1–7]. The significantly increased surface interaction area of PS can enhance the detection signal, in either fluorescence or electrical measurements. The characteristic photoluminescence (PL) of PS makes it a special functional material for colorimetric sensing. The mesoporous nanostructures of PS can reflect light and thus coupled biomolecules can be sensed by optical reflectivity to reveal the thickness change. Therefore, PS-based biosensors can be of significant use in medical, chemical, and bio-technology etc. In all biological applications, an interfacing biomolecular interaction is required for developing sensing devices. A stable and reproducible attachment of biomolecular probes on a surface, for the sensitive and specific capture of soluble receptors, is a prerequisite for following operations. An efficient immobilisation method must lead to a high surface coverage of biomolecules attached through a stable and easily formed linkage, while leaving a wide accessibility for the target molecule to enable biomolecular interactions. Although quite a few physical and chemical approaches have been employed to immobilise biomolecules, covalent grafting is mostly preferred because of the stability and reproducibility of the fabricated devices [8].

Among several organic molecules that can self-assemble on silicon surfaces and modify their intrinsic properties, silane molecules have been widely used [9] as an initial step to covalently attach adhesion promoters and cross linkers [9-12]. The silane 3-aminopropyltriethoxysilane (APTS) is one of the most common precursors [13] which, by following the appropriate process, can leave amine groups (NH_2) available for reaction with either a cross-linking agent or directly with a molecule and thus provides a reliable interface between biomolecules and a wide range of materials (Fig.4.1) [14-16].

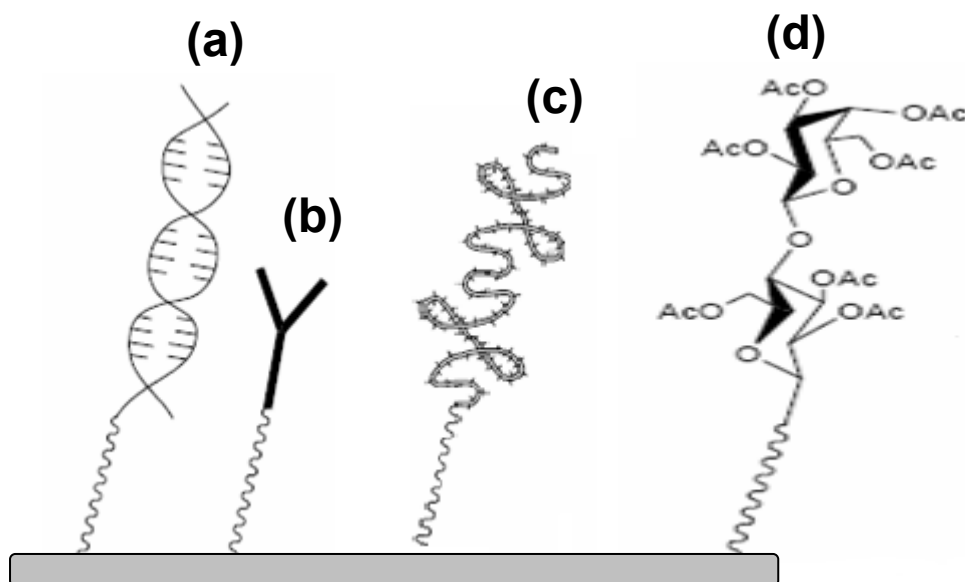


Figure 4.1. A selected number of functional groups that can be covalently attached to APTS modified silicon surfaces (a) DNA, (b) antibodies, (c) proteins, and (d) carbohydrates.

Silanes are attached through the formation of a Si-O-Si bond between the surface and the silanol groups. In addition to this covalent attachment, a broad range of available chemical functionalities at the other functional end of the silane molecules allows flexible adaptation of the surface for various applications. Particularly, APTS has been widely used because of its amino terminal group [17-20], which makes APTS especially attractive for biotechnology purposes such as DNA microarrays [21], protein arrays [22], and sol-gels. [23] APTS can form a covalently attached self-assembled film (SAM) on a wide variety of substrates [24-27] including hydroxyl-terminated silicon oxide substrates [25-27]. The reaction of the bond formation between the silicon oxide surface and the APTS molecules proceed with the hydrolysis of the alkoxy groups (first step) followed by the covalent adsorption of the resulting hydroxysilane (second step) [28]. The presence of water at the surface of the silicon surface is therefore necessary to catalyze the reaction as it is responsible for the first step of the reaction, but control of the moisture (physisorbed water layer) is key for the quality of the interface [12, 29].

In the present study, we report the surface functionalisation of nanostructured PS prepared at different current densities (I_d) 20 and 50 mAcm^{-2} , respectively. Here, the organic functionalisation of the PS surfaces was performed by APTS treatment. Furthermore, characterization of these organic monolayers by Fourier Transform Infrared spectroscopy (FTIR), X-ray photoelectron spectroscopy (XPS) and Photoluminescence

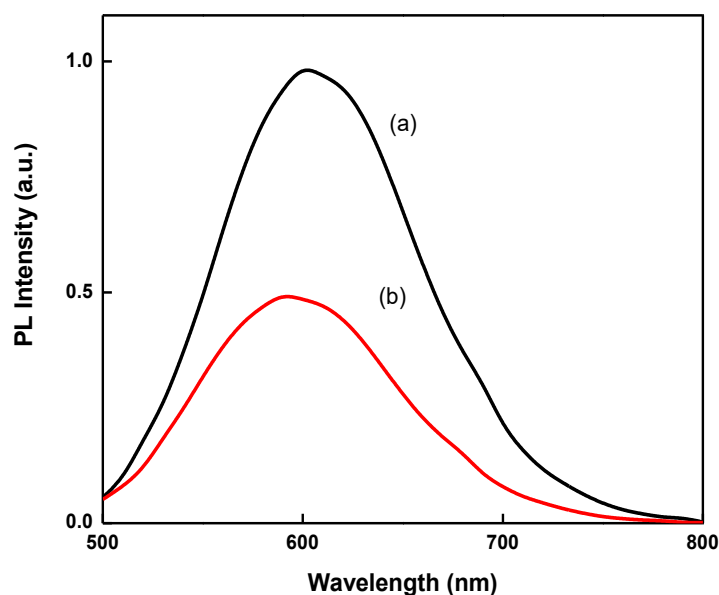


Figure 4.2 PL spectra of PS at $I_d \sim 20 \text{ mA cm}^{-2}$ (a) as-anodized and (b) APTS treated

Fig. 4.3 shows PL spectra of as anodised PS (Fig. 4.3 (a)) and APTS treated PS (Fig.4.3 (b)) prepared at $I_d \sim 50 \text{ mA cm}^{-2}$. The APTS treated PS film at $I_d \sim 20 \text{ mA cm}^{-2}$ shows PL quenching with decrease in PL intensity but less than APTS treated PS film prepared at $I_d \sim 50 \text{ mA cm}^{-2}$. Enhanced quenching in case of high porosity film ($I_d \sim 50 \text{ mA cm}^{-2}$) may be due to increased surface area for APTS adsorption. Upon APTS adsorption only PL intensity decreases but there is no shift in PL peak position which means that the porous morphology remains unaltered by silanization reaction.

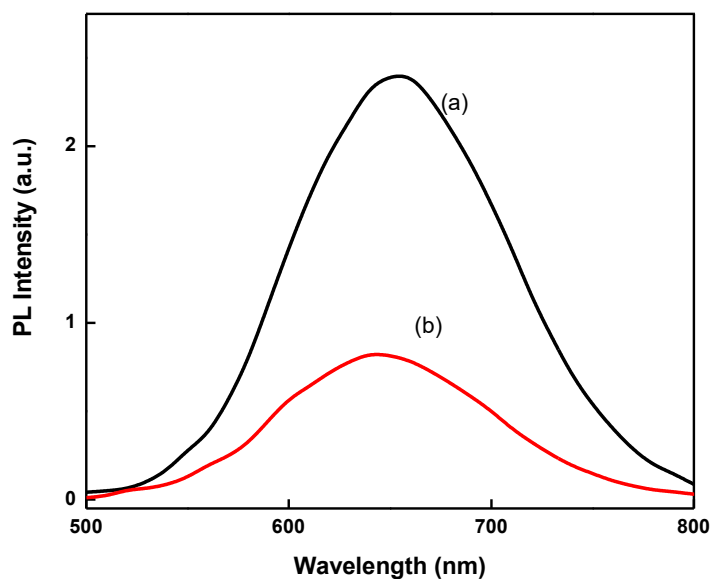


Figure 4.3 PL spectra of PS at $I_d \sim 50 \text{ mA cm}^{-2}$ (a) as-anodized and (b) APTS treated

Hydrogen-terminated PS surfaces, obtained by electrochemical etching in fluoride containing media, oxidize slowly in air, leading to slow degradation of photoluminescence (PL) and concomitant degradation of the electronic properties. Many studies have been focused on the formation of silicon oxide species under thermal, electrochemical, or chemical oxidation conditions to stabilize the H-terminated surface [6, 7]. The decay of PL intensity is a good indication of the stability of PS films particularly of surface bond configurations [2]. In Fig. 4.4, decay of the PL intensity at the peak wavelength under humid conditions for PS films formed as-anodized and APTS-treated PS at $I_d \sim 20$ (Fig. 4.4 (a) (b)) and 50 mA cm^{-2} (Fig. 4.4 (c)(d)), are compared. The PL peak position was recorded for different times corresponding to a fixed wavelength. As shown in Fig. 4.4, significant decay of the PL intensity is observed for fresh PS film as compared to the APTS treated films. Under humid conditions, the rate of PL decay for fresh PS film at $I_d \sim 20 \text{ mA cm}^{-2}$ is ~ 0.74 while in sample made at $I_d \sim 50 \text{ mA cm}^{-2}$ its value is ~ 0.71 . The rate of PL decay for APTS-treated PS prepared at 20 and 50 mA cm^{-2} are ~ 0.53 and 0.50 , respectively. The above results indicated that the formation of stable surface and correlates with the superior mechanical stability of APTS-treated PS films prepared at $I_d \sim 50 \text{ mA cm}^{-2}$ as compared to PS films formed at $I_d \sim 20 \text{ mA cm}^{-2}$ and fresh (as-anodised) PS film.

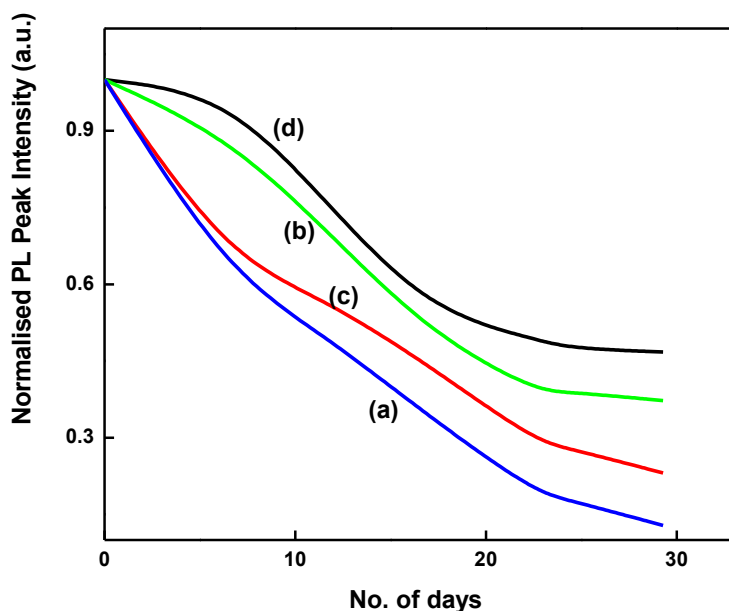


Figure 4.4. PL decay under humid condition (a) fresh PS and (b) APTS-treated PS at $I_d \sim 20 \text{ mA cm}^{-2}$ and (c) fresh PS and (d) APTS-treated PS corresponding to $I_d \sim 50 \text{ mA cm}^{-2}$

FTIR Studies

Fig. 4.5 (a-d) shows FTIR spectra of Fresh PS and APTS-treated PS corresponding to $I_d \sim 20 \text{ mA cm}^{-2}$. From Fig. 4.5 (a), for $I_d \sim 20 \text{ mA cm}^{-2}$, fresh PS surface shows the Si-H_x stretching mode at $\sim 2111 \text{ cm}^{-1}$, Si-H_x bending modes at ~ 907 and 630 cm^{-1} [32]. A weak signature of O atoms either bonded to Si at $\sim 1235 \text{ cm}^{-1}$ is visible. The FTIR spectrum of freshly (as anodised) prepared PS sample after exposure to humid conditions for 30 days is shown in Fig. 4.5 (b). The prominent increase in peak intensity $\sim 1250 \text{ cm}^{-1}$ may be due the presence of Si-O-Si mode under humid conditions but the intensity of hydride-terminated surface $\sim 2100 \text{ cm}^{-1}$ is only reduces marginally as compared with that of the freshly prepared sample. This indicates that the hydrolysis of the Si-H_x groups on the surface of PS is very difficult in a pure water [33]. IR spectrum of PS oxide surface (after SC2) exposed to APTS shows a band peaking near 1145 cm^{-1} (Figure 4.5 c). This band

correspond to a combination of Si-O-Si vibrational modes including those of bonds formed between the silane and oxide surface, cross-linking between silane molecules at the surface, polymerization of silane, and unreacted Si-O-C (ethoxy) groups[12]. Bands in the region of $2800\text{--}2990\text{ cm}^{-1}$ (centered at 2942 cm^{-1}) and the most prominent feature for all spectra is located

$\sim 1500\text{--}1700\text{ cm}^{-1}$ (centered near 1580 cm^{-1}) are assigned to CH_2 stretching and NH_2 bending, respectively [12, 34]. The above IR results prove that APTS had been grafted onto the PS surface. Fig. 4.5 (d) shows the IR spectrum of APTS treated PS under humid condition which shows a appreciably increase in oxide related species Si-O-Si ($1100\text{--}1200\text{ cm}^{-1}$) and decrease in the peak intensity of region $\sim 1500\text{--}1700\text{ cm}^{-1}$. The above IR spectra indicate that APTS treated PS is more stable than freshly prepared PS under humid condition.

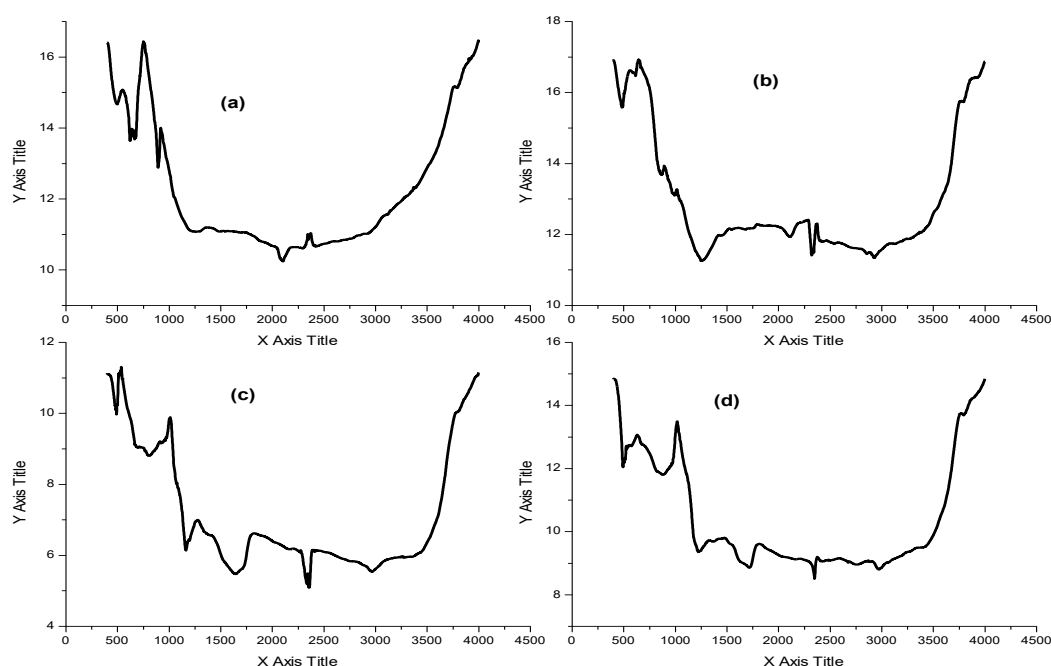
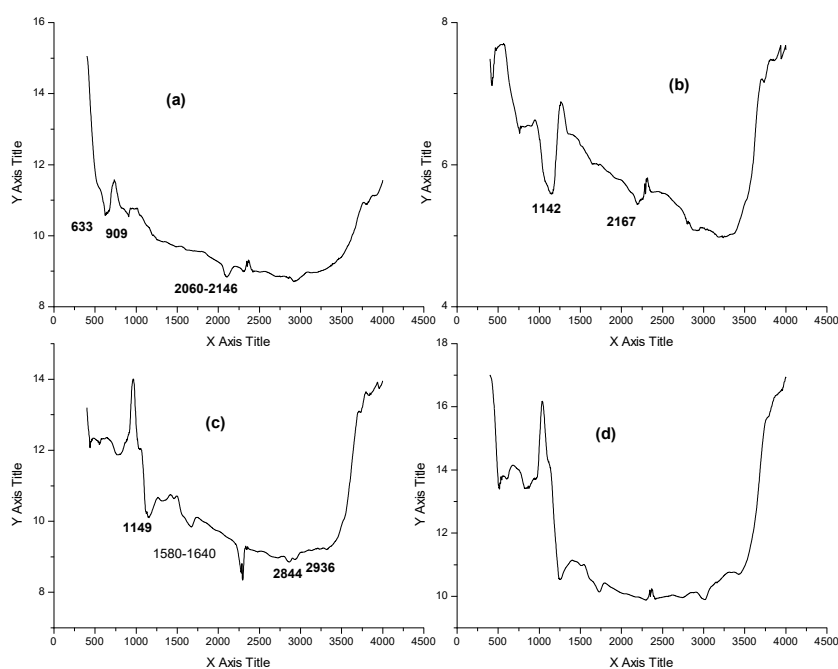


Figure 4.5 shows FTIR spectra of (a) Fresh PS, (b) Fresh PS under humid ambience, (c) APTS-treated PS and (d) APTS-treated PS under humid ambience corresponding to $I_d \sim 20\text{ mA cm}^{-2}$

Fig. 4.6 (a-d) shows the IR spectra of fresh PS and APTS-treated PS corresponding to $I_d \sim 50\text{ mA cm}^{-2}$. The IR spectrum of a freshly hydride-terminated PS is shown in **Fig. 4.6 (a)**. It exhibits a typical tripartite band for Si-Hx stretching modes $2060\text{--}2146\text{ cm}^{-1}$ (2060 cm^{-1} for Si-H, 2104 cm^{-1} for Si-H₂, and 2146 cm^{-1} for Si-H₃). The Si-Hx bending modes exhibit absorptions at 909 and 633 cm^{-1} , respectively [8]. Under humid conditions it is found that no obvious change in the absorptions related to Si-Hx vibrations of as prepared PS indicating that the hydrolysis of the Si-Hx on the surface of PS is negligible in the pure water atmosphere (Fig. 4.6 (b)). The appearance of a peak with higher intensity around 1142 cm^{-1} is indicative of Si-O-Si stretching mode under humid ambience due to oxidation. Other peak at $\sim 2900\text{ cm}^{-1}$ represents C-H stretching modes which is due to presence of hydrocarbon could be incorporated through slight atmospheric contamination of freshly prepared PS [7,35]. The hydrolysis of the H-terminated PS surfaces to form hydroxyl-terminated surfaces is accomplished for grafting biomolecules using a well-developed silanization process and subsequent chemical functionalization **Figure 4.6 (c-d)** shows the spectra characteristic of PS surface

functionalized with APTS molecules when the reaction is complete at room temperature and its stability study under humid conditions. Upon treatment of PS film with APTS the spectral region $\sim 900\text{--}1250\text{ cm}^{-1}$ involves the Si-O-Si stretching modes, including those formed by attachment of APTS to the oxide surface. However, in addition to the Si-O-Si stretching mode that originate from direct bonding of the APTS molecule to the SiO_2 surface, this spectral region also contains the SiO-C stretching mode and the SiO- CH_2CH_3 rocking mode. The IR spectrum of APTS-treated PS film as shown in **Fig. 4.6 (c)** shows presence of new peaks which are characterised by the aliphatic C-H stretching modes at ~ 2844 and 2936 cm^{-1} corresponding to CH_2 symmetric and asymmetric stretching modes respectively [12, 34, 36]. In **Fig. 4.6 (c)** IR absorption bands are observed at $\sim 1640\text{ cm}^{-1}$, assigned to the bending band of NH_2 and that at $\sim 1580\text{ cm}^{-1}$ to the bending band of protonated amines ($-\text{NH}_3^+$) [8, 37]. A weak peak at 1494 cm^{-1} is attributed to the C-H₂ deformation mode [38]. The corresponding N-H stretching vibration at 3300 cm^{-1} is more difficult to observe because of its weak dipole moment, and is often too weak to detect for film coverage [12]. Under humid conditions, the FTIR spectra of fresh PS film is modestly affected with the increased peak intensity of Si-O-Si related mode at $\sim 1219\text{ cm}^{-1}$ [12,13] and negligible decrease in NH_2 related species (**Fig. 4.6 (d)**). Thus, oxidation by means of humid conditions has not as much of effect on the properties of APTS-treated PS films which shows the chemical stability and inertness of PS films after APTS-treatment. These results are also supported by PL decay studies



as well.

Figure 4.6 FTIR spectra of (a) Fresh PS, (b) Fresh PS under humid ambience, (c) APTS-treated PS and (d) APTS-treated PS under humid ambience corresponding to $I_d \sim 50\text{ mA cm}^{-2}$

XPS Studies

XPS experiments are performed to elucidate the composition of molecule attached, the valence states of various element present and to determine the level of molecule attached. **Fig. 4.7 (a-d)** shows the full XPS survey spectra of fresh PS and APTS-treated PS films at $I_d \sim 20$ and 50 mA cm^{-2} . **Fig. 4.7 (a) and (b)** shows the XPS spectra of fresh PS films at $I_d \sim 20$ and 50 mA cm^{-2} , respectively both spectra displays the following

peaks at 284.6, 531.7, and a doublet at 99.0 and 102.9 eV corresponding to C (1s), O (1s) and Si (2p), respectively. [8, 38] After APTS treatment, N(1s) XPS signal at 401.3 eV appears in both cases may be attributed to incorporation of amines-NH₂ species on the surface of APTS-treated PS films Fig. 4(c) (d). The intensity of N (1s) signal is higher in PS sample prepared at $I_d \sim 50 \text{ mA cm}^{-2}$ (Fig 4.7 (c)) as compared to the PS sample prepared at $I_d \sim 20 \text{ mA cm}^{-2}$ (Fig 4.7 (d)) [8].

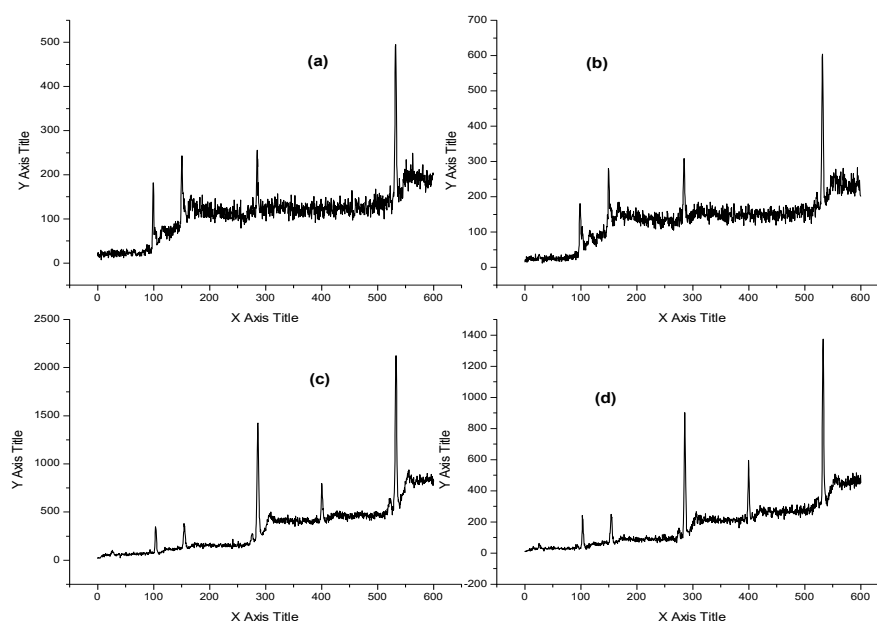


Fig. 4.7 XPS survey spectra of (a) fresh PS at $I_d \sim 20 \text{ mA cm}^{-2}$, (b) APTS-treated PS at $I_d \sim 20 \text{ mA cm}^{-2}$, (c) fresh PS at $I_d \sim 50 \text{ mA cm}^{-2}$, and (d) APTS-treated PS films at $I_d \sim 50 \text{ mA cm}^{-2}$

Fig. 4.8 shows the Si (2p) core-level XPS spectra for fresh PS, APTS-treated PS and their corresponding spectra under humid ambience. From **Fig. 4.8.1 (a)** and **Fig. 4.8.2 (a)** for fresh PS prepared at $I_d \sim 20$ and 50 mA cm^{-2} , respectively, the Si (2p) core level spectra shows the doublet at 99.0 and $\sim 103 \text{ eV}$ which indicates that Si exists in two different environments pure Si and oxidized Si, respectively [12].

Fig. 4.8.1 (b) and Fig. 4.8.2 (b) shows a reduction in Si (2p) spectra in the region of 99 eV peak for both lower ($I_d \sim 20 \text{ mA cm}^{-2}$) and higher porosity ($I_d \sim 50 \text{ mA cm}^{-2}$) PS films after treating with APTS. The Si (2p) spectra shows increase in 103 eV peak for PS film corresponding to $I_d \sim 50 \text{ mA cm}^{-2}$ (**Fig. 4.8.2 (b)**) as compared to APTS-treated PS prepared at $I_d \sim 20 \text{ mA cm}^{-2}$ (Fig. 4.8.1 (b)). Increase 103 eV peak area may be due to utilization of Si-O-Si bonds are utilized during silanization reaction which indeed is a measure of the amount of APTS adsorbed at the surface (which is also mentioned in FTIR studies section).

Under humid ambience, the Si(2p) XPS peak intensity corresponding to pure Si ($\sim 99.1 \text{ eV}$) decreases drastically for fresh PS films and this effect is felt more for low porosity PS film ($I_d \sim 20 \text{ mA cm}^{-2}$) as evident from Fig. 4.8.1(b). This result is in sharp contrast to that of APTS-treated PS which shows no appreciable change in Si-core level XPS peak intensity corresponding to pure Si ($\sim 99.1 \text{ eV}$) under humid ambience for both lower ($I_d \sim 20 \text{ mA cm}^{-2}$) and higher porosity ($I_d \sim 50 \text{ mA cm}^{-2}$) PS films. Under humid ambience, the reduction in the XPS peak intensity for pure silicon is higher for fresh PS films as compared to APTS-treated

PS films indicating higher degree of oxidation for fresh PS films as compared to APTS-treated PS films which is evident from the above results. Upon oxidation, the rate of decrease of XPS signal for Si(2p) core level is significant for fresh PS as compared to APTS-treated PS which shows that APTS-treated PS films are relatively stable under oxidation conditions as also elucidated by PL decay and FTIR results respectively [39].

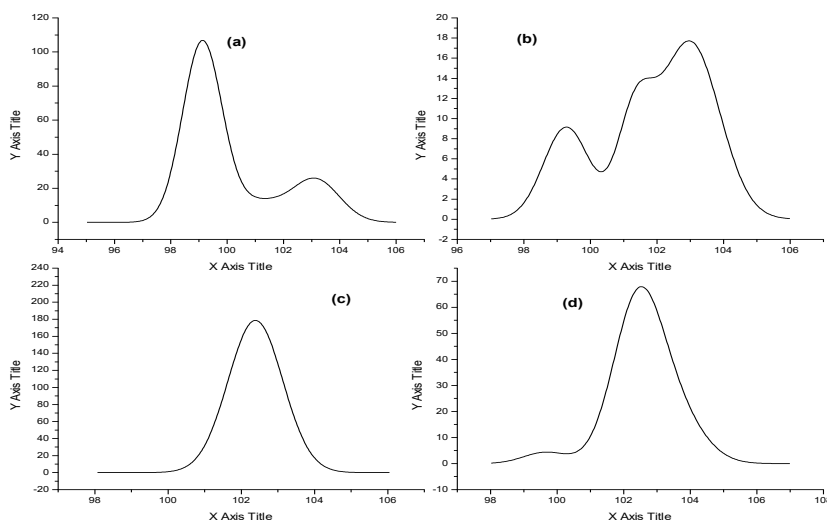


Fig. 4.8.1 Si (2p) core-level XPS spectra for (a) fresh PS, (b) fresh PS under humid ambience, (c) APTS-treated PS and (d) APTS-treated PS under humid ambience at $I_d \sim 20 \text{ mAcm}^{-2}$

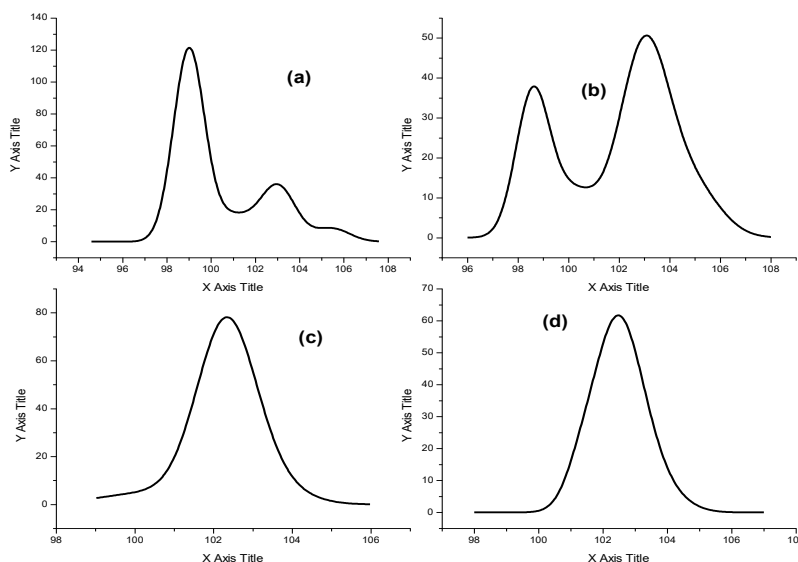


Fig. 4.8.2 Si (2p) core-level XPS spectra for (a) fresh PS, (b) fresh PS under humid ambience, (c) APTS-treated PS and (d) APTS-treated PS under humid ambience at $I_d \sim 50 \text{ mAcm}^{-2}$

Fig. 4.9 (Fig. 4.9.1 & Fig. 4.9.2) shows the O (1s) core-level XPS spectra for fresh PS, APTS-treated PS and their corresponding spectra under humid ambience corresponding to $I_d \sim 20$ & 50 mA cm^{-2} , respectively. From O(1s) core level spectra both fresh PS **Fig. 4.9.1 (a-b)** and APTS-treated PS **Fig. 4.9.2 (a-b)** films in normal

ambience exhibit similar XPS peak intensity at ~ 531.7 eV but under humid conditions, O(1s) peak corresponding to fresh PS (**Fig. 4.9.1 (c-d)**) shifts to higher binding energy (~ 532.2 eV) while O(1s) core-level intensity and peak position remains the same for APTS-treated PS film (**Fig. 4.9.2 (c-d)**) indicating higher level of oxidation for the former than for the latter. The effect of oxidation for fresh PS is severe for lower porosity sample (**Fig. 4.9.1 (d)**) as compared to higher porosity sample (**Fig. 4.9.1 (d)**) under humid conditions. From O (1s) core-level XPS spectra, it is evident that under humid conditions, APTS-treated PS film prepared at $I_d \sim 50 \text{ mA cm}^{-2}$ is quite stable which commensurates well with other XPS core-level and FTIR studies.

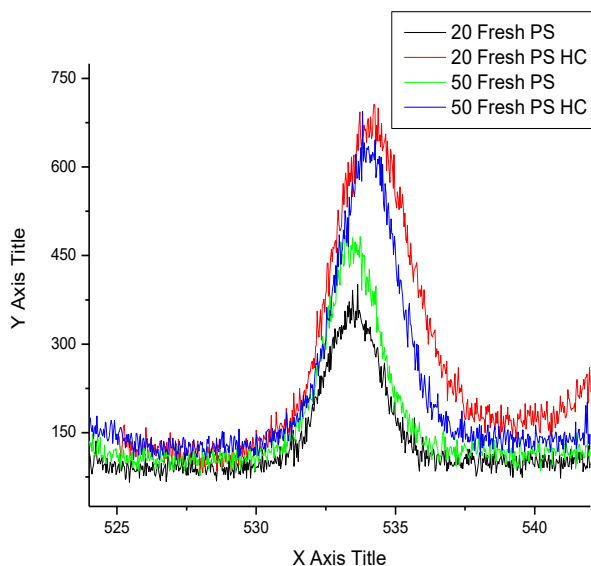


Fig. 4.9.1 O 1s core-level XPS spectra for fresh PS and fresh PS under humid ambience at $I_d \sim 20$ and 50 mAcm^{-2}

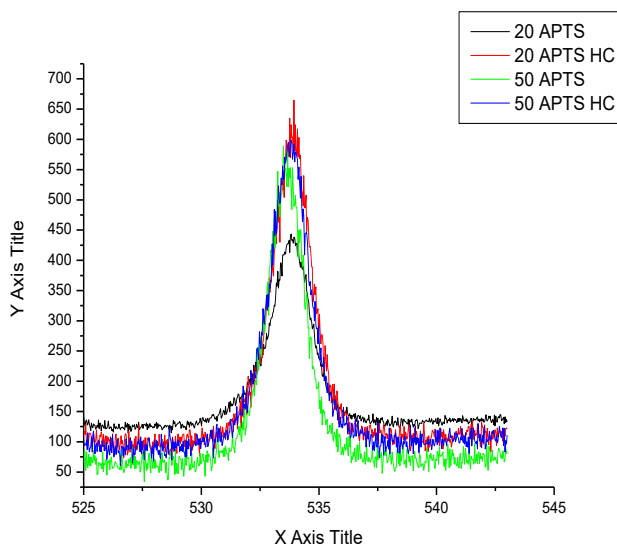


Fig. 4.9.2 O 1s core-level XPS spectra for APTS-treated PS and APTS-treated PS under humid ambience at $I_d \sim 20$ and 50 mAcm^{-2}

The C (1s) core-level XPS spectra corresponding to $I_d \sim 20$ & 50 mA cm^{-2} is shown in Fig. 4.10.1 and Fig. 4.10.2, respectively with peak at $\sim 284.6 \text{ eV}$ demonstrate that the fresh PS films exhibits lower carbon content as compared to APTS-treated PS films which can be attributed to an increase in C-like species (C and C-N) upon silanization. However, under humid conditions, C(1s) core-level intensity decreases marginally for APTS-treated PS film prepared at 50 mA cm^{-2} Fig. 4.10.2 (d) whereas the both fresh PS films shows a considerable increment in C(1s) XPS intensity possibly resulting from the atmospheric carbon contamination (Fig. 4.10.1(b) and Fig. 4.10.2 (b)).

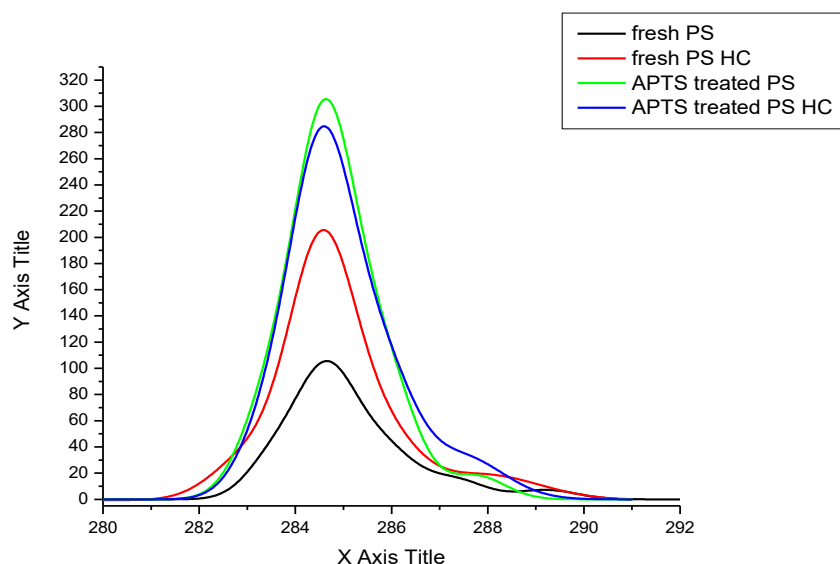


Fig. 4.10.1 C 1s core-level XPS spectra for (a) fresh PS, (b) fresh PS under humid ambience, (c) APTS-treated PS and (d) APTS-treated PS under humid ambience at $I_d \sim 20 \text{ mA cm}^{-2}$

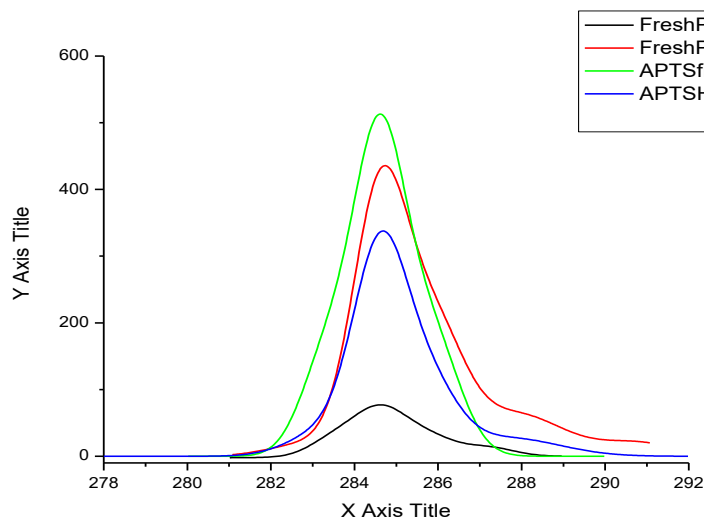


Fig. 4.10.2 C 1s core-level XPS spectra for (a) fresh PS, (b) fresh PS under humid ambience, (c) APTS-treated PS and (d) APTS-treated PS under humid ambience at $I_d \sim 50 \text{ mA cm}^{-2}$

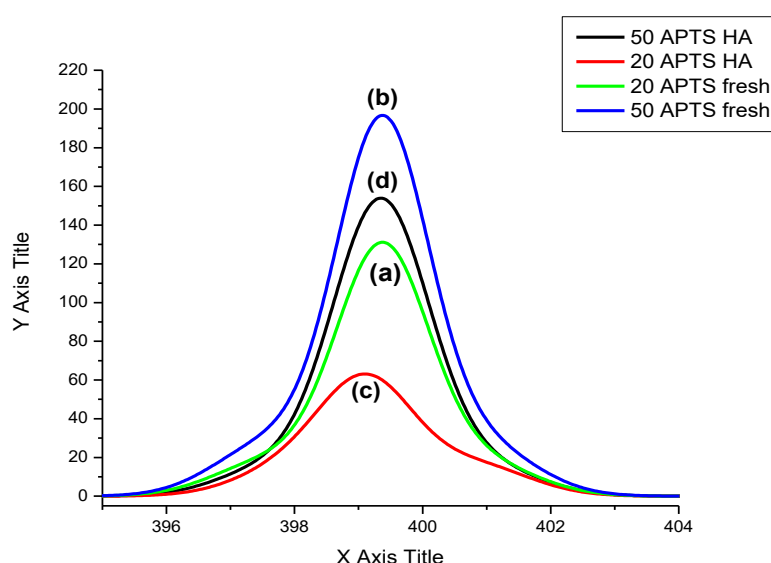


Fig. 4.11 N 1s core-level XPS spectra for APTS-treated PS and APTS-treated PS under humid ambience at $I_d \sim 20$ and 50 mA cm^{-2}

Fig. 4.11 (a-d) shows N (1s) core level XPS spectra corresponding to $I_d \sim 20$ & 50 mA cm^{-2} , respectively under normal and humid ambience. N(1s) core level XPS spectra shows a peak position at $\sim 399.0 \text{ eV}$ for both APTS-treated PS films ($I_d \sim 20$ & 50 mA cm^{-2}). The increment in N-signal with similar peak position in APTS-treated PS films prepared at $I_d \sim 50 \text{ mA cm}^{-2}$ (Fig. 4.11 (b)) as compared to APTS-treated PS films at $I_d \sim 20 \text{ mA cm}^{-2}$ (Fig. 4.11 (a)) indicates increment in NH_2 species on the surface of PS with large pore size this may provide large surface area resulting in better adsorption of APTS molecules. Under humid condition there is a decrease in N(1s) peak intensity which is more in case of PS film prepared at low current density PS film Fig. 4.11 (c) than the PS prepared at high current density (Fig. 4.11 (d)) and later is stable and resistant to oxidation. The absence of higher binding energy component here implies absence of any decomposition product of the APTS precursor.

Conclusion -

We have presented a simple silanization reaction to modify/functionalise PS surface prepared at two current densities $I_d \sim 20$ & 50 mA cm^{-2} . This reaction proceeds by hydrolysis of the surface silicon-hydrogen groups that generated hydroxyl-terminated surfaces from freshly prepared PS. The functionalization of the hydroxyl-terminated PS surface with silanization reagents proceeds by abstraction of SiO_2 to form an organic monolayer. The resulting monolayer is stable under a variety of humid condition and retains the intrinsic structural properties of the PS layers. Surface functionalisation of nanostructured PS films and their stability under humid condition are characterised using PL, FTIR and XPS techniques. PS films prepared at $I_d \sim 50 \text{ mA cm}^{-2}$, having high PL intensity and stable surface bond configurations, as compared to PS film prepared at $I_d \sim 20 \text{ mA cm}^{-2}$ confirms its viability for the effective biofunctionalisation using APTS as precursor which can ensure covalent linking between the surface and biomolecules. The ease of this method of biofunctionalisation and low cost technique opens the possibility of using biofunctionalised PS in biosensing devices, microarray technology, organic semiconductors, and many other biotechnology and physics applications.

Reference:-

1. M. J. Sailor and E. J. Lee, *Adv. Mater.*, 1997, 9, 783.
2. M. D. Stewart and J. M. Buriak, *Adv. Mater.*, 2000, 12, 859.
3. S. E. Letant and M. J. Sailor, *Adv. Mater.*, 2001, 13, 335
4. H. Sohn, S. Letant and M. J. Sailor, *J. Am. Chem. Soc.*, 2000, 122, 5399;
5. J. Wei, J. M. Buriak and G. Siuzdak, *Nature*, 1999, 39, 243;
6. A. G. Cullis, L. T. Canham and P. D. J. Calcott, *J. Appl. Phys.*, 1997, 82, 909.
7. Dongsheng Xu,* Lin Sun, Hongliang Li, Lei Zhang, Guolin Guo, Xinsheng Zhao and Linlin Gui, Hydrolysis and silanization of the hydrosilicon surface of freshly prepared porous silicon by an amine catalytic reaction, *New J. Chem.*, 2003, 27, 300–306.
8. Bing Xia,ab Shou-Jun Xiao,*ab Dong-Jie Guo,a Jing Wang,a Jie Chao,a Hong-Bo Liu,a Jia Pei,a Ya-Qing Chen,a Yan-Chun Tange and Jian-Ning Liu*c, Biofunctionalisation of porous silicon (PS) surfaces by using homobifunctional cross-linkers, *J. Mater. Chem.*, 2006, 16, 570–578.
9. Haller, I. *J. Am. Chem. Soc.* 1978, 100 (26), 8050-8055.
10. Witucki, G. L., *J. Coatings Technol.* 1993, 65 (822), 57-60.
11. Krupke, R.; Malik, S.; Weber, H. B.; Hampe, O. *Nano Letters* 2002, 2 (10), 1161-1164
12. Pasternack RM, Rivillon Amy S, Chabal YJ., Attachment of 3-(Aminopropyl)triethoxysilane on silicon oxide surfaces: dependence on solution temperature. *Langmuir*. 2008 Nov 18;24 (22):12963-71
13. V.A. Basyuk, A.A. Chuiko, *Z. Priklad. Spektrosk.* 52 (1990) 935.
14. H. Sigrist, A. Collioud, J.-F. Cle'mence, H. Gao, R. Luginbu"hl, M. Sa"nger, G. Sundarababu, *Opt. Eng.* 34 (1995) 2339.
15. L. Rexova'-Benkova', E. Stratilova', M. Capka, *Biocatalysis* 4 (1990) 219.
16. M. Arroyo-Herna'ndez, R.J. Marti'n-Palma *, V. Torres-Costa, J.M. Marti'nez Duart, Porous silicon optical filters for biosensing applications, *Journal of Non-Crystalline Solids* xxx (2006) xxx-xxx
17. Yamaura, M.; Camilo, R. L.; Macêdo, M. A.; Nakamura, M.; Toma, H. E. *J. Magn. Mater.* 2004, 279(2-3), 210-217
18. Taylor, A. P.; Webb, R. I.; Barry, J. C.; Hosmer, H.; Gould, R. J.; Wood, B. J. *J. Microsc.* 2000, 199 (1), 56–67
19. Rezania, A.; Johnson, R; Lefkow, A. R.; Healy, K. E. *Langmuir* 1999, 15, 6931-6939
20. Liu, Z.; Li, Z.; Zhou, H.; Wei, G.; Song, Y.; Wang, L. *J. Microsc.* 2005, 218(3), 233-239
21. Falsey, J. R.; Renil, M.; Park, S.; Li, S.; Lam, K. S. *Bioconjugate Chem.* 2001, 12(3), 346 -353
22. Doh, J.; Irvine, D. J. *PNAS* 2006, 103, 5700-5705
23. Mansur, H. S.; Vasconcelos, W. L.; Lenza, R. S.; Oréface, R. L.; Reis, E. F.; Lobato, Z. P. *J. Non-Crys. Solids* 2000, 273(1-3), 109-115
24. Kurth, D. G.; Bein, T. *Langmuir* 1995, 11, 3061-3067.
25. Arslan, G.; Özmen, M.; Gündüz, B.; Zhang, X.; Ersöz, M. *Turk. J. Chem.* 2006, 30, 203-210.

26. Simon, A.; Cohen-Bouhacina T.; Porté, M. C.; Aimé, J. P.; Baquey, C. J. *Colloid Interf. Sci.* 2002, 251, 278-283
27. Li, H.; Perkass, N.; Li, Q.; Gofer, Y.; Koltypin, Y.; Gedanken, A. *Langmuir* 2003, 19, 10409 -10413.
28. Blümel, J. J. *Am. Chem. Soc.* 1995, 117, 2112-2113
29. Kallury, K. M. R.; Macdonald, P. M.; and Thompson, M. *Langmuir* 1994, 10, 492-499.
30. S.N. Sharma, G. Bhagavannarayana, Umesh Kumar, R. Debnath, S. Chandramohan, *Physica E: Low-dimensional Syst Nanostruct* 36(1), 65 (2007)
31. S.E. Letant, B.R. Hart, S.T.A.C.I.R. Kane, M.Z. Hadi, S.J. Shields, J.G. Reynolds, *Adv. Mater.* 16, 689 (2004).
32. A. V. Rao, F. Ozanam and J. N. Chazalviel, *J. Electrochem. Soc.*, 1991, 138, 153.
33. Hong-Liang Li,* Ai-Ping Fu,† Dong-Sheng Xu, Guo-Lin Guo, Lin-Lin Gui, and You-Qi Tang, *In Situ Silanization Reaction on the Surface of Freshly Prepared Porous Silicon*, *Langmuir* 2002, 18, 3198-3202.
34. Socrates, G. *Infrared and Raman Characteristic Group Frequencies*, 3rd ed.; John Wiley & Sons Ltd: West Sussex, England, 2001.
35. P. Gupta, A. C. Dillon, A. S. Bracker and S. M. George, *Surf. Sci.*, 1991, 245, 360.
36. Norman A. Lapin† and Yves J. Chabal, *Infrared Characterization of Biotinylated Silicon Oxide Surfaces, Surface Stability, and Specific Attachment of Streptavidin*, *J. Phys. Chem. B* 2009, 113, 8776–8783
37. G. Shen et al. / *Colloids and Surfaces B: Biointerfaces* 35 (2004) 59–65
38. J.H. Song, M.J. Sailor, *J. Am. Chem. Soc.* 120, 2376 (1998)
39. Shalini Singha,b Shailesh N. Sharmaa, Govinda, Mukhtar A. Khanb and P.K. Singha, *Hydrosilylation of 1-dodecene on Nanostructured Porous Silicon Surface: Role of Current Density and Stabilizing Agent*, *Icopton*